Letters

A Tunable Power Sharing Control Scheme for the Output-Series DAB DC–DC System With Independent or Common Input Terminals

Nie Hou, *Student Member, IEEE*, and Yun Wei Li, *Senior Member, IEEE*

***Abstract*—To connect the low voltage energy storage source equipment and the medium voltage dc (MVdc) bus, the output-series dual-active-bridge (OS-DAB) dc–dc converter system with independent or common input terminals becomes a promising option. For the OS-DAB dc–dc converter system, this letter proposes a simple tunable power sharing control (TPSC) strategy to maintain the voltage of MVdc bus, manage power sharing ratio for each energy storage system. The proposed strategy allows energy storage equipment hot swap as well as converter system black start. Experimental results verify the analysis in this letter and the excellent performance of proposed TPSC strategy.**

***Index Terms*—Black start, energy storage system, hot swap, medium voltage dc (MVdc), power sharing control.**

I. Introduction

ALONG with the development of renewable energies such as wind turbine energy and solar energy [1], the dc power distribution system has been a promising alternative to collect, transfer, and distribute these energies. Since these power sources always generate unstable electrical power, energy storage source (ESS) system has become an essential technology to boost robustness and stability of dc power distribution system [2]. The ESS components such as batteries and super capacitors always offer low output voltage. Therefore, the output-series dc–dc converters with independent or common input terminals and modular multilevel converter isolated dc–dc converter system can be employed to connect the low voltage dc (LVdc) component and the medium voltage dc (MVdc) bus [3]–[5].

For the output-series dc–dc converter, there are some strategies dealing with the voltage sharing performance for input-series structure [6], [7]. These strategies usually focus on the input side of converter system, and the output voltage sharing is naturally allocated by obeying the energy law. Therefore, these schemes are not completely suitable for the output-series dc–dc converters with independent or common input terminals. Moreover, based on proportional and integral (PI) controller, some methods are presented to address the output voltage sharing performance for input-parallel-output-series dc–dc converter [8], [9], but these strategies restrict the dynamic responses of the output-series dc–dc converter system without accurate adjustment of capacitor voltages.

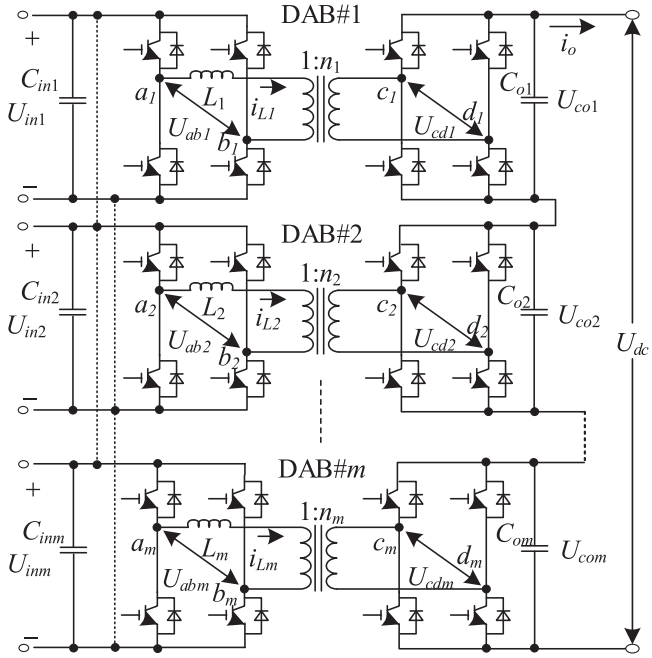

Fig. 1. Topology of the OS-DAB dc–dc converter system.

Since the output-series dual-active-bridge (OS-DAB) dc–dc converter is adopted widely to link LVdc bus and MVdc bus in dc power system [11], [12], the OS-DAB dc–dc converter with independent or common input terminals as shown in Fig. 1 is studied in this letter. Generally, in dc power system, the OS-DAB dc–dc converter system with ESS system should meet various controlling requirements, such as the following:

1) The uninterrupted power supply for maintaining the output dc-link voltage.
2) The tunable power sharing ability for state-of-charge-balancing control of different ESS equipment.
3) The hot swap control of multiple ESS system for maintenance and replacement of ESS equipment.

Manuscript received December 15, 2018; revised January 29, 2019; accepted April 2, 2019. Date of publication April 14, 2019; date of current version June 28, 2019. *(Corresponding author: Nie Hou.)*

The authors are with the Department of Electrical and Computer Engineering, University of Alberta, Edmonton, AB T6G 2V4, Canada (e-mail: nhou@ualberta.ca; yunwei.li@ualberta.ca).

Color versions of one or more of the figures in this letter are available online at http://ieeexplore.ieee.org.

Digital Object Identifier 10.1109/TPEL.2019.2911059

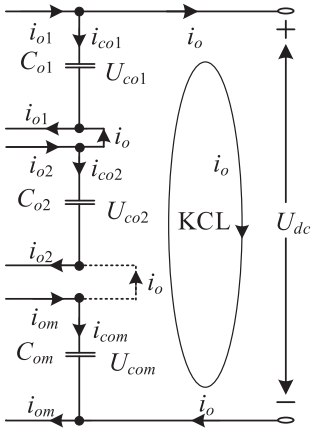

Fig. 2. Output-side circuit of the OS-DAB dc–dc converter system.

4) The back-start performance for reducing fluctuations of output capacitor voltages during startup process.

Therefore, this letter proposes a tunable power sharing control (TPSC) strategy for the OS-DAB dc–dc converter system with independent or common input terminals to meet all the requirements. Experimental results from a hardware prototype of the OS-DAB dc–dc system with two DAB modules verify the excellent performances of the proposed TPSC scheme.

II. TPSC Strategy With Black-Start and Hot-Swap Abilities

A. Proposed TPSC Strategy

For output-series converter systems, the power sharing performance is determined by the output-capacitor voltage values $U_{co\alpha}$ of each converter as

$$P_1{:}P_2{:}\ldots{:}P_m = U_{co1} : U_{co2} \ldots : U_{\rm com}. \tag{1}$$

Therefore, the power sharing performance of the OS-DAB dc–dc converter can be realized by adjusting $U_{co\alpha}$. Moreover, the relationship between the change in capacitor voltage $\Delta U_{co\alpha}$ and the charging current $i_{co\alpha}$ in a switching period T_s is described as [13]

$$i_{co\alpha} = \frac{\Delta U_{co\alpha} C_{o\alpha}}{T_s} \tag{2}$$

where $C_{o\alpha}$ is the output capacitor for each DAB module. In addition, the output-side circuit of the OS-DAB converter system is shown in Fig. 2. In Fig. 2, the current flowing between two close DAB converters is equivalent to i_o according to Kirchhoff's Current Law. Then, the output current of each DAB module $i_{o\alpha}$ is expressed as follows:

$$i_{o\alpha} = i_o + i_{co\alpha}. \tag{3}$$

Moreover, the transferred current $i_{T\alpha}$ of DAB dc–dc converter based on single-phase-shift method is shown as [14]

$$i_{T\alpha} = \frac{P_\alpha}{U_{co\alpha}} = \frac{U_{\rm in\alpha} D_\alpha (1 - |D_\alpha|) T_s}{2 n_\alpha L_\alpha} \tag{4}$$

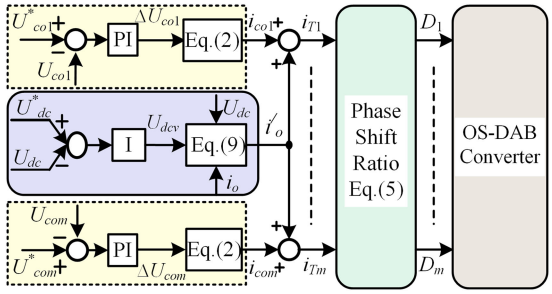

Fig. 3. Block schematic of the TPSC strategy.

where P_α is the transferred power, $U_{\rm in\alpha}$ is the input voltage, D_α is the phase-shift ratio, n_α is the transformer turn ratio, and L_α is the inductance for each DAB dc–dc module. Then, D_α is calculated by $i_{T\alpha}$ as

$$\begin{cases} D_\alpha = \frac{1}{2} - \sqrt{\frac{1}{4} - \frac{2 n_\alpha L_\alpha i_{T\alpha}}{U_{\rm in\alpha} T_s}} & (i_{T\alpha} \geq 0) \\ D_\alpha = -\frac{1}{2} + \sqrt{\frac{1}{4} + \frac{2 n_\alpha L_\alpha i_{T\alpha}}{U_{\rm in\alpha} T_s}} & (i_{T\alpha} < 0). \end{cases} \tag{5}$$

Ignoring power losses, the transferred power is equivalent to the output power of each DAB module, and $i_{T\alpha}$ will be equivalent to $i_{o\alpha}$. However, the power losses of the OS-DAB dc–dc converter in actual system cannot be neglected. Therefore, a compensation coefficient k_C should be introduced to eliminate the difference between $i_{o\alpha}$ and $i_{T\alpha}$ as

$$i_{T\alpha} = k_C i_{o\alpha}. \tag{6}$$

In terms of accurately maintaining output dc-link voltage of the OS-DAB dc–dc converter, k_C can be calculated by a virtual output voltage $U_{{\rm dc}v}$ generated by the outer-voltage loop integral controller with the control input ($U^*_{\rm dc} - U_{\rm dc}$). Then, k_C is expressed as

$$k_C = \frac{U_{{\rm dc}v}}{U_{\rm dc}}. \tag{7}$$

According to (7), (3) can be further expressed as

$$i_{T\alpha} = \frac{U_{{\rm dc}v}}{U_{\rm dc}} i_o + \frac{U_{{\rm dc}v}}{U_{\rm dc}} i_{co\alpha}. \tag{8}$$

As shown in (8), $i_{T\alpha}$ can be divided into two parts for meeting the output-current requirement for load and adjusting capacitor voltage for each DAB dc–dc converter as

$$\begin{cases} i'_o = \frac{U_{{\rm dc}v}}{U_{\rm dc}} i_o \\ i'_{co\alpha} = \frac{U_{{\rm dc}v}}{U_{\rm dc}} i_{co\alpha} \approx i_{co\alpha}. \end{cases} \tag{9}$$

In (9), when desired output dc-link voltage of the OS-DAB dc–dc converter is achieved, $U_{{\rm dc}v}$ is approximately equal to $U_{\rm dc}$. Therefore, in terms of adjusting the capacitor voltage for each DAB converter, $i'_{co\alpha}$ can be seen as $i_{co\alpha}$. Then, combining (2) and (9), the block schematic of the TPSC strategy is shown in Fig. 3. As shown in Fig. 3, the TPSC strategy for the OS-DAB dc–dc converter system can be implemented. The I controller is employed to compensate the error between $U_{\rm dc}$ and $U^*_{\rm dc}$, and the PI controllers with the identical integral and proportionality

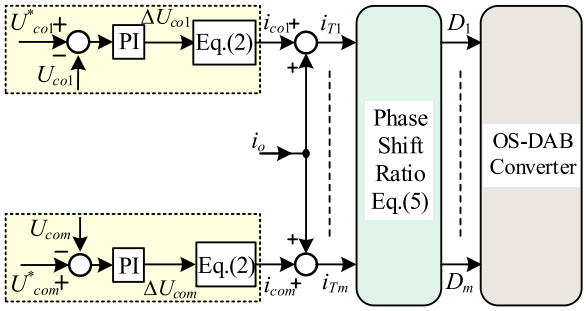

Fig. 4. Block schematic of the variant TPSC strategy for black start.

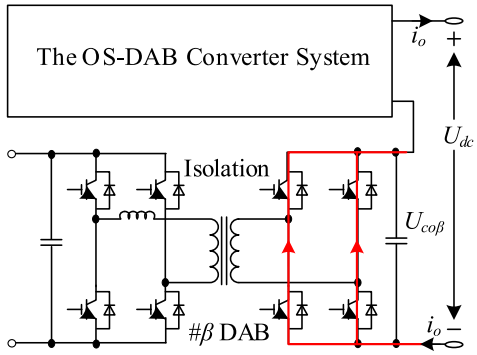

Fig. 5. Current flowing condition when one DAB module is bypassed.

parameters are used to adjust $U_{co\alpha}$ synchronously. At the beginning of each switching cycle, $U_{\mathrm{in}\alpha}$, $U_{co\alpha}$, and i_o are measured, and U_{dc} can be calculated as the sum of $U_{co\alpha}$. Through the PI controller, $\Delta U_{co\alpha}$ can be obtained by $U_{co\alpha}$ and $U^*_{co\alpha}$, and then, $i_{co\alpha}$ can be calculated according to (2). Similarly, from the I controller, $U_{\mathrm{dc}v}$ can be obtained by U_{dc} and $U^*{}_{\mathrm{dc}}$, and then, i'_o can be acquired by using (9). Finally, according to (5), D_α for each DAB module can be obtained. Generally, in the battery- or supercapacitor-based ESS system, $U^*_{co\alpha}$ can be acquired for implementing the state-of-charge-balancing control of batteries and super capacitors [15]–[17].

B. Black Start of the OS-DAB DC–DC System

Under the TPSC strategy, fluctuations of capacitor voltages are difficult to avoid, since the change of i'_o cannot be consistent with the change of i_o during startup process, and extra power will be employed to charge capacitor voltages. To realize black start of the OS-DAB dc–dc converter, a variant TPSC strategy should be used, as shown in Fig. 4.

Different from the original TPSC strategy, i_o is employed as a current feedforward control, and then, the load current can be satisfied continuously during the startup process. Therefore, the change of $U_{co\alpha}$ can be synchronized. When $U^*{}_{\mathrm{dc}}$ is reached, $U_{\mathrm{dc}v}$ in TPSC scheme can be calculated as

$$U_{\mathrm{dc}v} = U_{\mathrm{dc}}. \tag{10}$$

Based on (10), the variant TPSC scheme can be switched into TPSC scheme smoothly.

C. Hot-Swap Process of the ESS Equipment

To repair or replace energy storage equipment such as the battery and the super capacitor, the soft plug-in and plug-out control of DAB module is crucial for the OS-DAB dc–dc converter system. When the βth ESS equipment is required to be plugged out, the process is divided into two steps for plugging out this source: first, controlling the corresponding capacitor voltage close to zero, second, shorting out the corresponding second-side H-bridge of corresponding DAB module. During the first step, the capacitor voltage $U_{co\beta}$ should be reduced gradually based on the TPSC scheme. When $U_{co\beta}$ is smaller than the limited value U_{LM}, the switches of the second-side H-bridge can be turned ON, and U_{LM} can be expressed as

$$U_{LM} < i_{LM} R_{\mathrm{on}} \tag{11}$$

where i_{LM} is current rating of employed switches and R_{on} is the corresponding conducting resistor. Then, this DAB module can be bypassed, as shown in Fig. 5, and the corresponding energy storage equipment can be taken down.

In addition, when a new energy storage equipment is to be plugged in the OS-DAB dc–dc system again, the plug-in process can be implemented by using TPSC strategy with the new power sharing ratio for each DAB dc–dc module. Then, when the desired power sharing performance is achieved, this energy storage module can be plugged in completely.

D. Additional Applications of the TPSC Scheme

The basic operating principle of the proposed TPSC strategy is the accurate compensation of the load current and the precise adjustment of the capacitor voltages. Therefore, the relationship of the transferred current and the control value of the dc–dc converter module should be determined, such as in (4) for the DAB dc–dc converter. Then, according to this principle, the proposed method can be employed for the output-series dc–dc converter system with ac-inductance-based converter module. For the ac-inductance-based converter such as half-bridge dc–dc converter [18], full bridge dc–dc converter [19], and three-phase DAB dc–dc converter [20], the ac voltages are generated on both sides of its inductance resulting in ac inductance current. Then, the transferred power and transferred current of this kind converter can be determined by the control value in each switching period directly [21]. For example, the transferred current i_{TF} of full bridge dc–dc converter system can be expressed as

$$i_{TF} = \begin{cases} \frac{(nU_{\mathrm{in}F} - U_{\mathrm{o}F})U_{\mathrm{in}F}d^2}{4n_F f_F L_F U_{\mathrm{o}F}} & (0 < \varphi \le \frac{U_{\mathrm{o}F}}{nU_{\mathrm{in}F}}) \\ \frac{U_{\mathrm{in}F}}{8n_F f_F L_F} d(2-d) - \frac{U^2_{\mathrm{o}F}}{8n^3_F U_{\mathrm{in}F} f_F L_F} & (\frac{U_{\mathrm{o}F}}{nU_{\mathrm{in}F}} < \varphi \le 1) \end{cases} \tag{12}$$

where $U_{\mathrm{in}F}$ is input voltage, n_F is the transformer turn ratio, f_F is the switching frequency, L_F is the inductance, U_{oF} is the output voltage, and d is the phase-shift ratio for the full bridge dc–dc converter system. Each i_{TF} can be determined by a certain phase-shift ratio d. Based on (12), d can be calculated by i_{TF} and the TPSC strategy can be also implemented.

TABLE I
CIRCUIT PARAMETERS OF THE OS-DAB DC–DC CONVERTER

U_{in1}, U_{in2}	30 V
n_1, n_2	1/2
L_1	400 μH
L_2	200 μH
T_s	0.1 ms
R	40 Ω or 56 Ω
C_{o1}	1.0 mF,
C_{o2}	0.5 mF
U^*_o	60 V
f_s	10 kHz

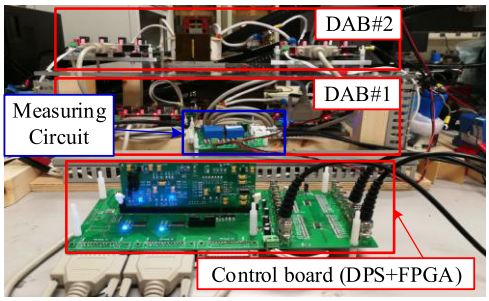

Fig. 6. Small-scale experimental platform for OSDAB dc–dc converter system with two modules.

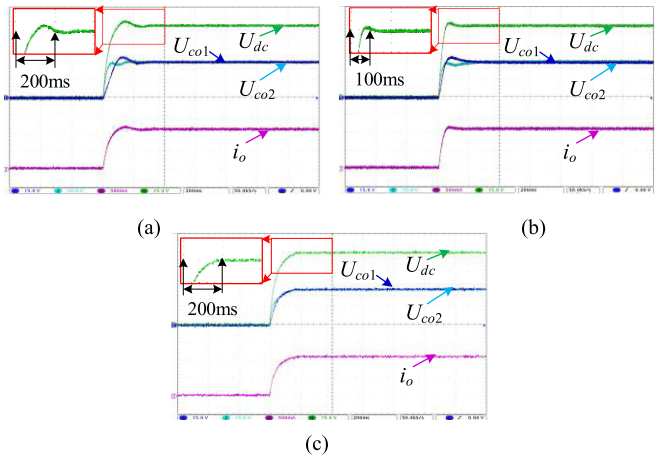

Fig. 7. Experimental results of startup process under different methods. (U_{co1}, U_{co2}, and $U_{\rm dc}$: 15 V/div; i_o: 0.5 A/div; time: 200 ms/div.) (a) VPI method. (b) TPSC strategy. (c) Variant TPSC scheme.

III. EXPERIMENT VERIFICATION

An experiment platform for the OS-DAB dc–dc converter system with two DAB modules is established to compare with the voltage PI-based (VPI) method and the TPSC scheme, and the main circuit parameters of the OS-DAB dc–dc converter are illustrated in Table I. The corresponding experimental platform is shown in Fig. 6.

When R is selected as 56 Ω, Fig. 7 shows the startup process of the OS-DAB dc–dc converter system under different strategies.

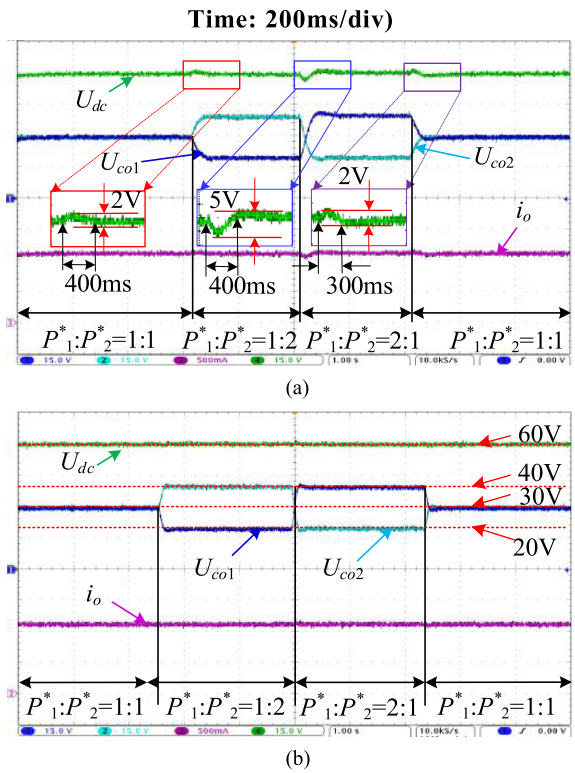

Fig. 8. Experimental results under changes of the power sharing requirement. (U_{co1}, U_{co2}, and $U_{\rm dc}$: 15 V/div; i_o : 0.5 A/div; time: 1 s/div.) (a) VPI method. (b) TPSC strategy.

As shown in Fig. 7, TPSC strategy can reach $U^*_{\rm dc}$ in a short time as 100 ms, compared with VPI method (200 ms) and variant TPSC scheme (200 ms). Moreover, based on the variant TPSC scheme, $U_{\rm dc}$, U_{co1}, and U_{co2} can obtain their desired values simultaneously, and the black-start performance of the OS-DAB dc–dc converter can be implemented.

When R is set to 56 Ω, Fig. 8 shows the experimental results under disturbances of power sharing coefficients. When the power sharing requirement is set as $P^*_1 : P^*_2 = 1 : 1$, U_{co1} and U_{co2} in steady-state condition should be stabilized at 30 and 30 V, respectively, and when output power of one DAB module is required as double as the output power of the other DAB module, its output voltage should also be twice the other's output voltage. As shown in Fig. 8(a), the disturbances of $U_{\rm dc}$ are bigger than 2 V during the adjusting process of U_{co1} and U_{co2} under VPI method, and the settling time of $U_{\rm dc}$ is about 400 ms for a new power sharing performance. Moreover, based on the TPSC strategy, $U_{\rm dc}$ can stay stable when adjusting U_{co1} and U_{co2} [see Fig. 8(b)].

When R is set to 56 Ω, Fig. 9 shows the experimental results during plug-out and plug-in processes of the second DAB module (representing the second ESS equipment). As shown in Fig. 9(a), when the second DAB module is plugged out or plugged in, the disturbance of $U_{\rm dc}$ is bigger than 4 V under VPI method, and the settling time for both processes is greater than 100 ms. Moreover, as shown in Fig. 9(b), regardless of plug-out process or plug-in process, $U_{\rm dc}$ can be maintained at its desired using the presented TPSC strategy.

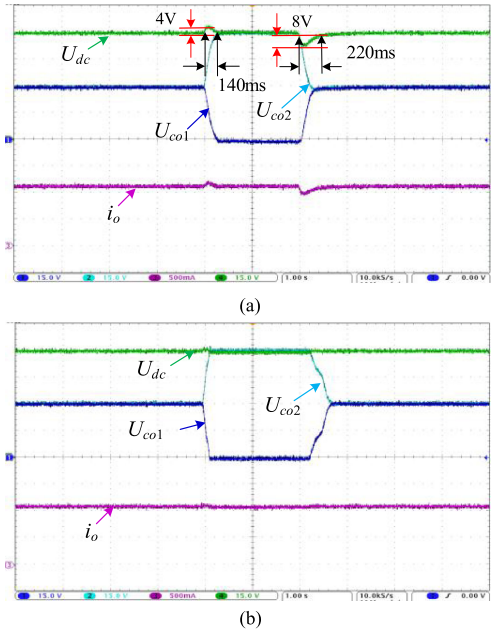

Fig. 9. Experimental results during the hot swap process. (U_{co1}, U_{co2}, and $U_{\rm dc}$: 15 V/div; i_o : 0.5 A/div; time: 1 s/div.) (a) VPI method. (b) TPSC strategy.

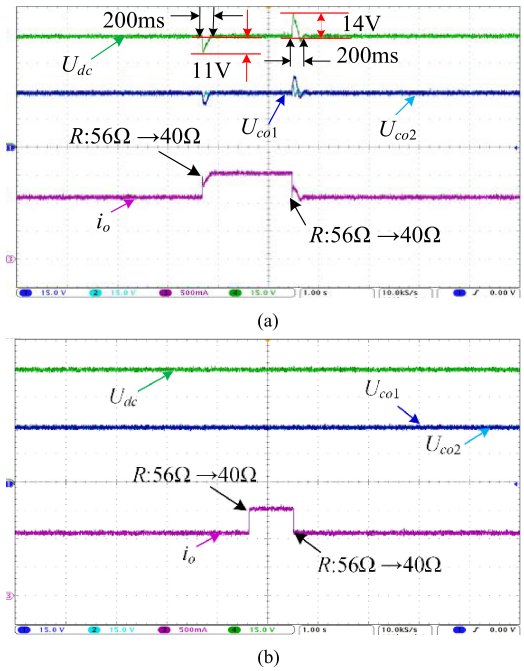

Fig. 10. Experimental results under disturbances of load resistor. (U_{co1}, U_{co2}, and $U_{\rm dc}$: 15 V/div; i_o : 0.5 A/div; time: 1 s/div.) (a) VPI method. (b) TPSC strategy.

Fig. 10 shows experimental results of the OS-DAB dc–dc converter under various load resistors between 40 and 56 Ω. As shown in Fig. 10(a), disturbances of $U_{\rm dc}$, U_{co1}, and U_{co2} are present under VPI method, and change in $U_{\rm dc}$ is close to 12 V. Moreover, the settling time of $U_{\rm dc}$ is about 200 ms. In addition, based on the TPSC strategy, $U_{\rm dc}$, U_{co1}, and U_{co2} are maintained at their desired values under TPSC scheme [see Fig. 10(b)], and the high robustness for the OS-DAB dc–dc converter can be provided.

IV. Conclusion

The OS-DAB dc–dc converter system is a promising option to connect LVdc components and MVdc bus for dc–dc system. In this letter, a TPSC strategy is proposed for the OS-DAB dc–dc converter system to deal with disturbance of load resistor, different power sharing performances, and even plug-in and plug-out requirements. Based on the proposed TPSC strategy, the conducted studies are summarized as follows:

1) The flexible power sharing performance can be achieved, and during the adjusting process of capacitor voltages, the output-side total voltage can be kept stable.
2) With a simple variation, the TPSC strategy can implement black-start performance for the OS-DAB dc–dc converter.
3) The plug-in and plug-out requirements can be satisfied, and when one DAB module is plugged in or plugged out, the output-side total voltage can stay unchanged.
4) The excellent dynamic responses under load resistor change can be achieved, and the capacitor voltages and the total voltage can also be maintained at their desired values during disturbances in the load condition.
5) According to the operating principle, the TPSC strategy can be employed for other output-series dc–dc converter system with ac-inductance-based dc–dc module.

References

[1] F. Blaabjerg, R. Teodorescu, M. Liserre, and A. V. Timbus, "Overview of control and grid synchronization for distributed power generation systems," *IEEE Trans. Ind. Electron.*, vol. 53, no. 5, pp. 1398–1409, Oct. 2006.
[2] F. Nejabatkhah and Y. W. Li, "Overview of power management strategies of hybrid ac/dc microgrid," *IEEE Trans. Power Electron.*, vol. 30, no. 12, pp. 7072–7089, Dec. 2015.
[3] Q. Song, B. Zhao, J. Li, and W. Liu, "An improved dc solid state transformer based on switched capacitor and multiple-phase-shift shoot-through modulation for integration of LVdc energy storage system and MVdc distribution grid," *IEEE Trans. Ind. Electron.*, vol. 65, no. 8, pp. 6719–6729, Aug. 2018.
[4] I. A. Gowaid, G. P. Adam, A. M. Massoud, S. Ahmed, and B. W. Williams, "Hybrid and modular multilevel converter designs for isolated HVdc–dc converters," *IEEE J. Emerg. Sel. Topics Power Electron.*, vol. 6, no. 1, pp. 188–202, Mar. 2018.
[5] Z. Xing, X. Ruan, H. You, X. Yang, D. Yao, and C. Yuan, "Soft-switching operation of isolated modular dc/dc converters for application in HVdc Grids," *IEEE Trans. Power Electron.*, vol. 31, no. 4, pp. 2753–2766, Apr. 2016.
[6] L. Qu, D. Zhang, and Z. Bao, "Active output-voltage-sharing control scheme for input series output series connected dc–dc converters based on a master slave structure," *IEEE Trans. Power Electron.*, vol. 32, no. 8, pp. 6638–6651, Aug. 2017.
[7] Q. Wei, B. Wu, D. Xu, and N. R. Zargari, "Model predictive control of capacitor voltage balancing for cascaded modular dc–dc converters," *IEEE Trans. Power Electron.*, vol. 32, no. 1, pp. 752–761, Jan. 2017.
[8] A. Darwish, D. Holliday, and S. Finney, "Operation and control design of an input-series–input-parallel–output-series conversion scheme for offshore dc wind systems," *IET Power Electron.*, vol. 10, no. 15, pp. 2092–2103, 2017.
[9] K. G. Anjana, M. Aniruddha Kamath, and M. Barai, "A differential current compensation technique for PV systems under partially shaded condition," in *Proc. IEEE Int. Conf. Compat., Power Electron. Power Eng.*, Cadiz, Spain, 2017, pp. 116–120.
[10] S. Lee, Y. Jeung, and D. Lee, "Output voltage regulation of IPOS modular dual active bridge dc/dc converters using sliding mode control," in *Proc. IEEE Appl. Power Electron. Conf. Expo.*, San Antonio, TX, USA, 2018, pp. 3062–3067.

[11] M. Stieneker and R. W. De Doncker, "Dual-active bridge dc–dc converter systems for medium-voltage dc distribution grids," in *Proc. IEEE 13th Brazilian Power Electron. Conf., 1st Southern Power Electron. Conf.*, Fortaleza, Brazil, 2015, pp. 1–6.

[12] T. Todorčević, R. van Kessel, P. Bauer, and J. A. Ferreira, "A modulation strategy for wide voltage output in DAB-based dc–dc modular multilevel converter for DEAP wave energy conversion," *IEEE J. Emerg. Sel. Topics Power Electron.*, vol. 3, no. 4, pp. 1171–1181, Dec. 2015.

[13] N. Hou, W. Song, Y. Li, Y. Zhu, and Y. Zhu, "A comprehensive optimization control of dual-active-bridge dc–dc converters based on unified-phase-shift and power-balancing scheme," *IEEE Trans. Power Electron.*, vol. 34, no. 1, pp. 826–839, Jan. 2019.

[14] R. W. A. A. De Doncker, D. M. Divan, and M. H. Kheraluwala, "A three-phase soft-switched high-power-density dc/dc converter for high-power applications," *IEEE Trans. Ind. Appl.*, vol. 27, no. 1, pp. 63–73, Jan./Feb. 1991.

[15] L. Maharjan, S. Inoue, H. Akagi, and J. Asakura, "State-of-charge (SOC)-balancing control of a battery energy storage system based on a cascade PWM converter," *IEEE Trans. Power Electron.*, vol. 24, no. 6, pp. 1628–1636, Jun. 2009.

[16] K. Bi, L. Sun, Q. An, and J. Duan, "Active SOC balancing control strategy for modular multilevel super capacitor energy storage system," *IEEE Trans. Power Electron.*, vol. 34, no. 5, pp. 4981–4992, May 2019.

[17] Y. Zhang and Y. Wei Li, "Energy management strategy for supercapacitor in droop-controlled dc microgrid using virtual impedance," *IEEE Trans. Power Electron.*, vol. 32, no. 4, pp. 2704–2716, Apr. 2017.

[18] H. Li, F. Z. Peng, and J. S. Lawler, "A natural ZVS medium-power bidirectional dc–dc converter with minimum number of devices," *IEEE Trans. Ind. Appl.*, vol. 39, no. 2, pp. 525–535, Mar./Apr. 2003.

[19] A. J. B. Bottion and I. Barbi, "Input-series and output-series connected modular output capacitor full-bridge PWM dc–dc converter," *IEEE Trans. Ind. Electron.*, vol. 62, no. 10, pp. 6213–6221, Oct. 2015.

[20] S. P. Engel, N. Soltau, H. Stagge, and R. W. De Doncker, "Dynamic and balanced control of three-phase high-power dual-active bridge dc–dc converters in dc-grid applications," *IEEE Trans. Power Electron.*, vol. 28, no. 4, pp. 1880–1889, Apr. 2013.

[21] W. Song, N. Hou, and M. Wu, "Virtual direct power control scheme of dual active bridge dc–dc converters for fast dynamic response," *IEEE Trans. Power Electron.*, vol. 33, no. 2, pp. 1750–1759, Feb. 2018.